THE JOURNAL OF PHYSICAL CHEMISTRY Letters

Letter

Cite This: J. Phys. Chem. Lett. 2018, 9, 745−750

pubs.acs.org/JPCL

Signatures of Conformational Dynamics and Electrode-Molecule Interactions in the Conductance Profile During Pulling of Single-Molecule Junctions

Leopoldo Mejía,[†] Nicolas Renaud,[‡] and Ignacio Franco*[,†,§]

[†]Department of Chemistry, University of Rochester, Rochester, New York 14627-0216, United States

[‡]Netherlands eScience Center, Science Park 140 1098 XG Amsterdam, The Netherlands

[§]Department of Physics, University of Rochester, Rochester, New York 14627-0216, United States

Supporting Information

ABSTRACT: We demonstrate that conductance can act as a sensitive probe of conformational dynamics and electrode−molecule interactions during the equilibrium and nonequilibrium pulling of molecular junctions. To do so, we use a combination of classical molecular dynamics simulations and Landauer electron transport computations to investigate the conductance of a family of Au-alkanedithiol-Au junctions as they are mechanically elongated. The simulations show an overall decay of the conductance during pulling that is due to a decrease in the through-space electrode-molecule interactions, and that sensitivity depends on the electrode geometry. In addition, characteristic kinks induced by level alignment shifts (and to a lesser extent by quantum destructive interference) were also observed superimposed to the overall decay during pulling simulations. The latter effect depends on the variation of the molecular dihedral angles during pulling and therefore offers an efficient solution to experimentally monitor conformational dynamics at the single-molecule limit.

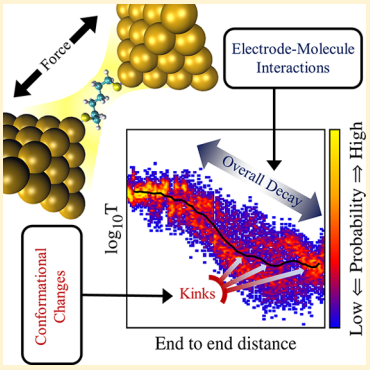

Understanding the electromechanical behavior of single molecules has become an important objective for the design of molecular electronic devices and the understanding of molecular junction properties.[1−15] In molecular junctions, electromechanical processes are used to monitor and control junction evolution,[8,16] provide a powerful platform to develop multidimensional single molecule spectroscopies,[17] and are used to develop mechanically activated electronic devices[18,19] or current-triggered mechanical actuators.[20,21]

Here we focus on experiments that combine single molecule pulling with electron transport measurements. In these experiments,[22−27] a molecule is covalently bonded to metallic electrodes that are slowly moved away from each other, inducing a mechanical stress on the molecular structure. Throughout the experiment, a bias voltage is applied across the junction, allowing measurement of the electronic current flowing through the molecule. Typically,[22,24−27] the conductance profile during elongation shows an initial decay due to the breaking of the metal−metal contact, before one or multiple plateaus are reached, signaling the formation of a metal-molecule-metal junction. The molecule subsequently detaches from one electrode, breaking the electronic connections and ending the experiment. Experiments usually[22,23,28−32] focus on the conductance plateau associated with the fully elongated molecule to characterize the junction and study physical or chemical processes,[22−24,28,29,33] while the electromechanical response of the molecule during its elongation is less commonly investigated.[17,19,25,27,34,35]

Here we computationally investigate the information content in the conductance of molecular junctions during their mechanical elongation in a family of alkanedithiols linking gold electrodes. We show that the overall decay of the conductance during pulling arises due to a decrease in through-space electrode−molecule interactions. In turn, we associate additional fine features or kinks observed in the conductance profile during pulling with changes of the molecular dihedrals. Such a connection between conformational changes and conductance in the context of alkane-based junctions has been encountered before,[26,34,36,37] but its physical origin is unclear. Here we demonstrate that this connection is due to changes in the energy of the frontier molecular orbitals induced by dihedral rotation. The simulations show that the conductance profile during pulling offers a sensitive probe of electrode−molecule conformational dynamics in equilibrium and nonequilibrium molecular ensembles, and highlight the potential utility of molecular junction measurements as a route to develop single-molecule spectroscopies.

The simulations were performed using an in-house modification of TRANSpull.[38] In these simulations, classical molecular dynamics (MD) of the pulling of Au(111)-alkanedithiol-Au(111) junctions were performed in the NVT ensemble using TINKER 7.1,[39] as schematically shown in Figure 1a. The dynamics was propagated using the modified Beeman

Received: December 15, 2017
Accepted: January 25, 2018
Published: January 25, 2018

DOI: 10.1021/acs.jpclett.7b03323
J. Phys. Chem. Lett. 2018, 9, 745−750

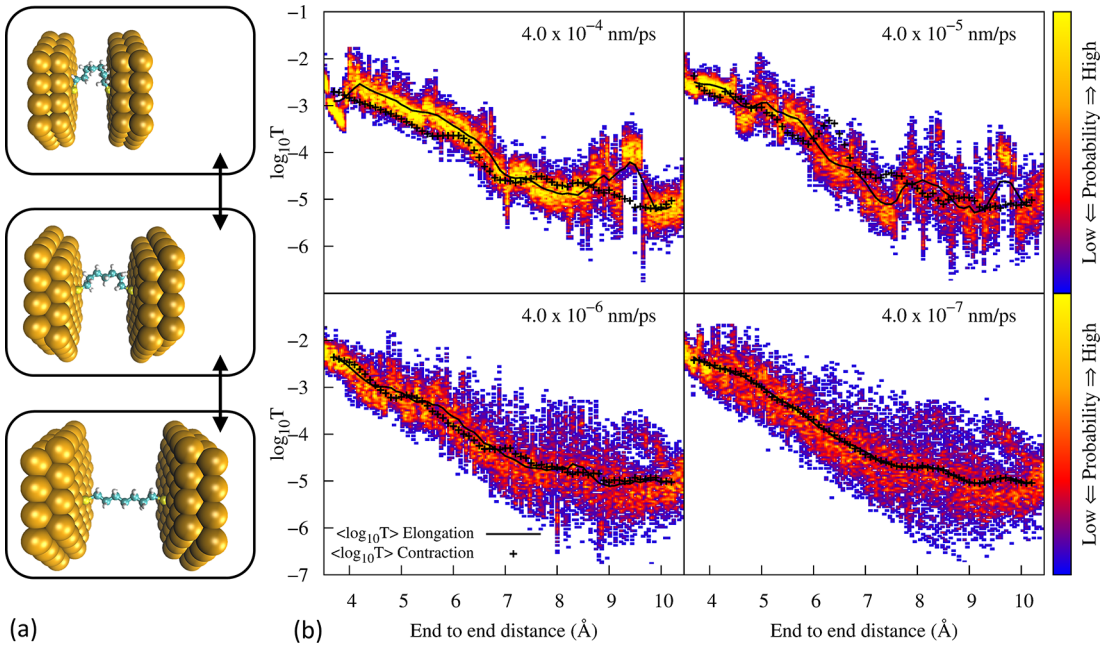

Figure 1. (a) Schematic representation of the pulling of a molecular junction. Both electrodes are truncated Au(111) flat surfaces. The alkanes are bonded to the electrodes through thiol bonds at the fcc position. (b) Effect of pulling speed on the probability density distribution of the transmission coefficient $T(E_F)$ of Au(111)-S-$(CH_2)_7$-S-Au(111) system. The solid lines represent the average of $\log_{10} T(E_F)$ during the elongation and the crosses represent the average of $\log_{10} T(E_F)$ during the contraction. The probability distribution shown correspond to the elongation process. The range of the color scale in the probability density was chosen in each case such that all molecular events would be visible. Equilibrium behavior is achieved for a pulling speed of 4.0×10^{-7} nm/ps, where the transmission during pulling and subsequent contraction essentially coincide.

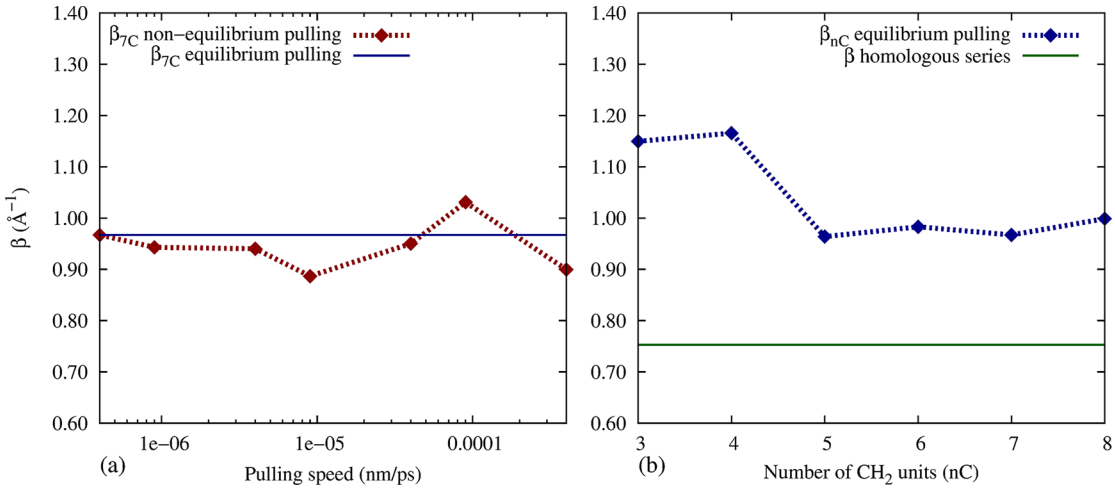

Figure 2. Tunneling decay coefficients during pulling β_{nC} versus pulling speed and molecular length. (a) Tunneling decay coefficient β_{7C} for the equilibrium and nonequilibrium pullings of the Au(111)-S-$(CH_2)_7$-S-Au(111) junction. (b) Tunneling decay coefficient β_{nC} as a function of molecular length; the β obtained from the homologous series of fully elongated alkanedithiols is included (solid green line) for comparison purposes. The variation of β_{nC} with respect to pulling speed and molecular length is small (RSD equal to 0.05 and 0.09, respectively), which suggest that β_{nC} is not an intrinsic molecular property.

algorithm[40,41] with a 1 fs integration time and a Nosé−Hoover chain at 298 K as a thermostat.[42−44] MM3 was selected as a force field because it properly describes the behavior of alkanethiols.[45−47] To mimic the effects of the electrode surfaces on the MD, we built two parallel hexagonal-shaped double layer surfaces made of impenetrable dummy atoms arranged in a Au(111) pattern. The hexagonal surfaces have a side length of 8.65 Å and a maximal diameter of 17.30 Å. The terminal sulfur atoms were attached to a stiff isotropic harmonic potential that mimicked the chemical bond to the surface at the fcc position and fixed the S−Au distance to 2.35 Å, as described in the literature.[48] At initial time, the end-to-end (sulfur to sulfur) distance in the molecule, is chosen to be 3.5 Å for all the pulling simulations. To mimic the pulling, one electrode is moved away from the molecule at a constant speed. The pulling direction is defined by a vector perpendicular to the electrode surfaces. The molecules were pulled until the potential energy increases abruptly due to deformation of the molecular backbone. Subsequently, the transmission at the Fermi energy $T(E_F)$, which is proportional to the conductance in the low bias limit $G = \frac{2e^2}{h} T(E_F)$,[1,49] was computed with TRANSpull[38] using

DOI: 10.1021/acs.jpclett.7b03323
J. Phys. Chem. Lett. 2018, 9, 745−750

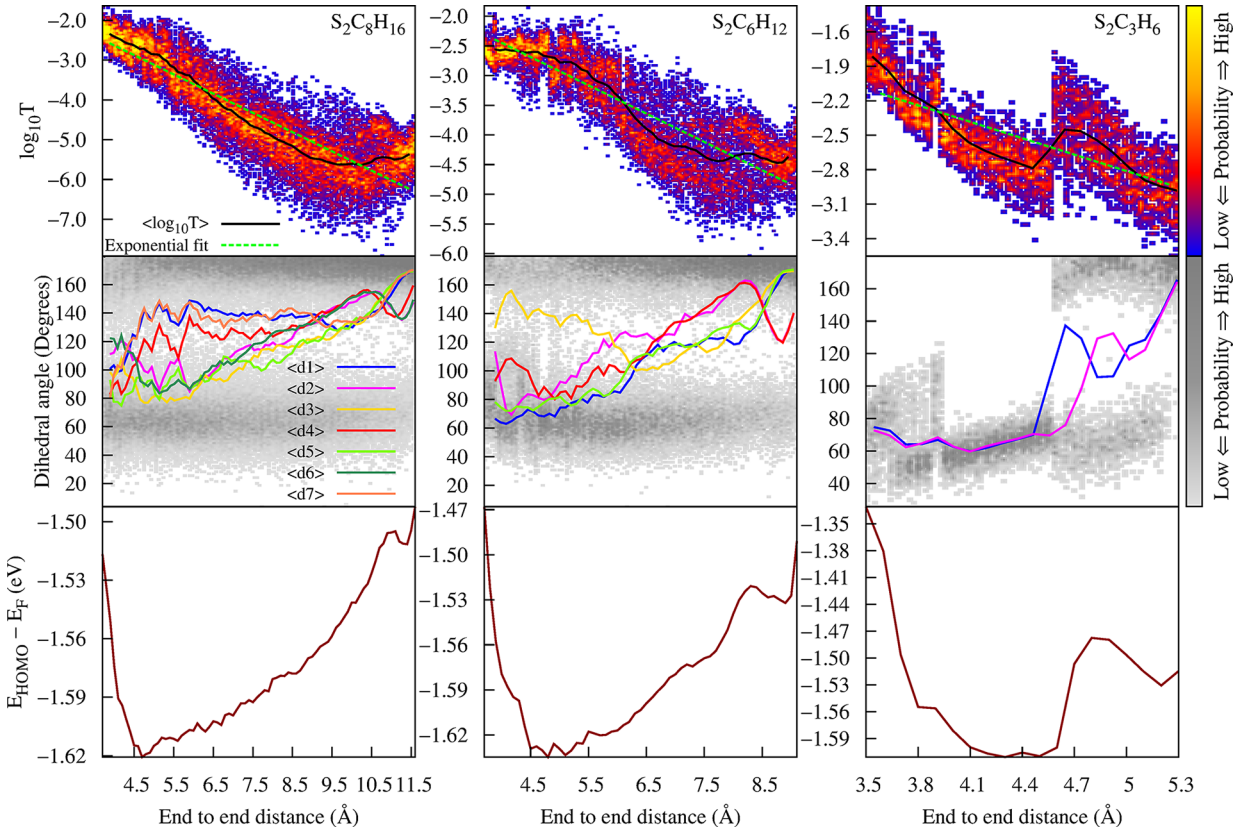

Figure 3. Transmission, variation of dihedral angles, and change of the $E_{HOMO} - E_F$ energy gap during the equilibrium pulling of three representative alkanedithiols (C_8, C_6 and C_3). Upper panels: Probability density distribution of the transmission as a function of end-to-end distance (black lines indicate averages). Middle panels: Average value of the dihedrals among carbon atoms in the chain (colored lines) and their collective distribution (gray dots) during elongation. The dihedrals are labeled consecutively along the chain. The first and last dihedral include the terminal thiol group. Bottom panels: Average variation of the $E_{HOMO} - E_F$ energy gap with respect to the end-to-end distance. Note that the generation of gauche conformations during pulling leads to dips in the transmission due to changes in the HOMO alignment. This correlation makes the transmission a sensitive probe of conformational dynamics.

nonequilibrium Green's functions[50] for molecular conformations reached during the pulling. The electronic structure of the junction was modeled using an extended Hückel formalism,[51] because it captures the essential electronic couplings and enables the simulations of several thousand conformations at a reasonable computational cost. While the density of states of the electrodes was considered in the wide band limit approximation,[52] bilayers of gold atoms were explicitly introduced in the simulations to define the electrode-molecule couplings. The zero-bias conductance was computed using the 6s Au orbital energy as the Fermi level (E_F) for 2000 snapshots per Å of pulling, and the resulting statistical set was used to obtain averages.

One of the challenges in simulating single molecule pulling processes is the 6−12 orders of magnitude disparity between experimental and computational pulling speeds. Here we overcome this problem by using pulling speeds slow enough to get reversible behavior, where the transmission during elongation and contraction essentially coincide and the simulation is considered to be in the equilibrium regime. Figure 1b shows the effect of the pulling speed on the probability density distribution of the transmission coefficient of the Au(111)-S-$(CH_2)_7$-S-Au(111) system during elongation and contraction. The equilibrium pulling is reached for a pulling speed of 4.0×10^{-7} nm/ps; at this point the simulations recover the equilibrium behavior where results become independent of the pulling speed. The broad distribution of conductance values under equilibrium conditions are due to thermal fluctuations of the junction. The width of the conductance distribution during nonequilibrium conditions reflects the conformational space visited by the molecule during pulling. Note that, as seen in Figure 1b, the zero bias conductance exhibits kinks along the pulling superimposed to an overall decay.

We observe that the overall conductance decay is due to a decrease of through-space molecule-electrode interactions and, surprisingly, not due to changes in molecular conformation during pulling. The first evidence for this claim comes from the examination of the transmission versus elongation for different pulling speeds. During equilibrium pulling, the molecule samples all accessible conformational space, while during nonequilibrium conditions the conformations encountered during pulling depend on the initial conditions. Figure 2a shows the values of the tunneling decay coefficient β_{7C} during the pulling of the Au(111)-S-$(CH_2)_7$-S-Au(111) junction for different pulling speeds, obtained by fitting the transmission to the exponential function $T = T_0 e^{-\beta_{nC} d}$, where d corresponds to the end-to-end distance during the pulling and β_{nC} is the tunneling decay coefficient during the pulling of the corresponding alkanedithiol with a molecular chain of n carbons. While the decay of the conductance during pulling is not necessarily exponential, to be able to compare our results with the literature, throughout we choose to use the exponential form as a qualitative descriptor of the decay. As shown, the observed overall decay of the conductance is very similar for equilibrium and

DOI: 10.1021/acs.jpclett.7b03323
J. Phys. Chem. Lett. 2018, 9, 745−750

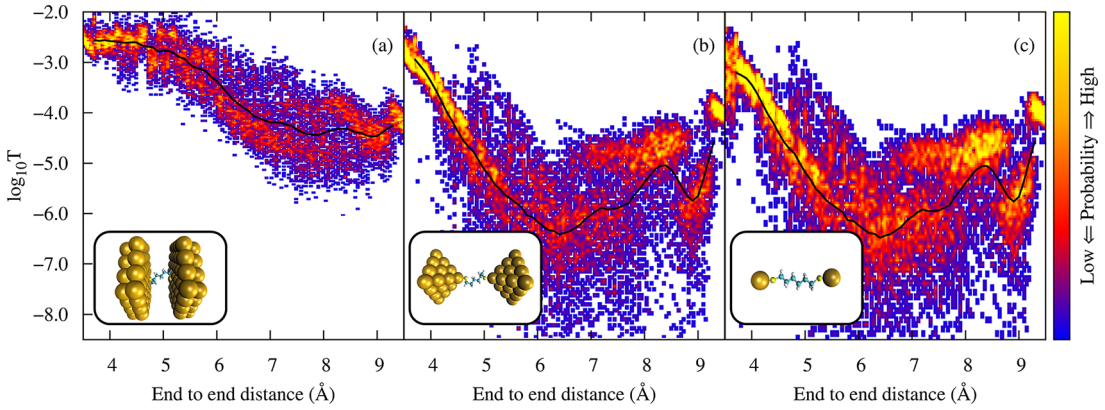

Figure 4. Probability density distribution of the transmission as a function of the end-to-end distance of the $S_2C_6H_{12}$ alkanedithiol (black lines indicate averages) using different electrode shapes: (a) flat Au(111), (b) pyramidal Au cluster, and (c) single Au atom. The sharper the electrode, the weaker the electrode−molecule interactions. Note that the overall decay of the conductance changes when the strength of the electrode−molecule interactions change.

nonequilibrium simulations. In fact, the β_{7C} values are around 0.95 $Å^{-1}$ and largely insensitive to the pulling speeds (relative standard deviation (RSD) of 0.05), indicating that the details of the molecular conformations encountered during pulling do not influence the overall conductance decay.

To further show that the decay coefficient β_{nC} is not an intrinsic molecular property but that it depends on changes of electrode−molecule interactions, we computed the equilibrium transmission versus elongation of S-$(CH_2)_n$-S (n = 3−8) alkanedithiols in the Au(111) junction. Note that by keeping the same electrode and the same kind of molecules, the electrode−molecule interactions are expected to be comparable. The top panels of Figure 3 contain the probability density distribution of the transmission as a function of the end-to-end distance for three representative cases. In all cases (n = 3−8), the transmission profile shows an overall decay along the pulling accompanied by some kinks. The resulting tunneling decay coefficients β_{nC} are shown in Figure 2b. As can be seen, the values of β_{nC} are around 1.00 $Å^{-1}$ and exhibit only a mild dependence with system size (RSD of 0.09). Notably, for the larger molecules (n = 5−8) the β_{nC} coefficient is highly independent of the molecular length (RSD of 0.02).

The fact that the equilibrium β_{nC} coefficients do not change appreciably with the molecular chain size, along with their independence with pulling speed, strongly suggests that the tunneling decay coefficient during pulling is not an intrinsic molecular property but that it depends on electrode−molecule interactions. To demonstrate this, we changed the electrode shape during the transport while keeping the same equilibrium molecular dynamics trajectory for the S-$(CH_2)_6$-S pulling. As shown in Figure 4 the overall decay of the transmission strongly depends on the shape of the electrode. Hence, a modification of the electrode−molecule interactions result in a significant change in the overall decay of the conductance. This is important to consider when examining experimental results, as this component of the electron transport is sensitive to junction geometry. Additional computations shown in Figure S1 (Supporting Information) show that through-space electrode-molecule couplings are responsible for the overall decay, except for very short distances where through-space intramolecular interactions also play a significant role.

Contrary to the hypothesis in ref 35, we find that the β_{nC}'s coefficients shown in Figure 2b do not numerically coincide with the tunneling decay coefficient β (solid green line in Figure 2), obtained by doing computations in the homologous series of fully elongated molecules and fitting the transmission versus molecular length D to the exponential function $T = T_0e^{-\beta D}$. The reason for this is that, unlike β, the physical origin of the β_{nC} is determined by electrode−molecule interactions and not by intrinsic molecular properties. Hence, β and β_{nC} are unrelated quantities.

In contrast with the overall decay, our results demonstrate that the fine features or kinks in the transmission are related to the conformational dynamics of the molecule in the junction. In fact, Figure 1b shows that the kinks in the transmission strongly depend on the pulling speed and thus on the details of the ensemble encountered during elongation. Furthermore, the pattern of kinks encountered for a given molecule does not qualitatively change when changing the electrode geometry (see Figure 4). In addition, comparing the conformational dynamics of the molecule with the conductance (Figure 3) reveals a qualitative connection between the kinks and the evolution of dihedrals during pulling, as we explain below. The middle panels of Figure 3 shows the evolution of the dihedral angles during pulling for three representative molecules. The distribution of dihedral angles behaves like a bimodal function in which each dihedral angle can adopt either a gauche conformation (~60°) or an anti conformation (~180°). A clear example of the connection between the conductance and the molecular conformation is provided by the kink in the transmission for the $S_2C_3H_6$ alkanedithiol. This kink is due to removal of gauche defect by pulling. This connection is also seen in longer molecules, albeit somewhat obscured by other competing processes.

The changes of the conductance due to changes in the molecular dihedral angles can be tracked to level alignment during pulling. Specifically, the bottom panels of Figure 3 shows the average variation of the energy of the HOMO along the pulling for these three representative cases. Here, the transmission is governed by hole transport through the HOMO, which dominates charge transport in alkanes.[2] A comparison between the bottom, middle, and top panels of Figure 3 shows a qualitative correlation between the kinks in the transmission, the conformational changes and the variation of the energy of the HOMO. Thus, the sensitivity of the conductance to dihedral angles arise because changing the dihedrals changes the energy of the MO's responsible for the transport.

DOI: 10.1021/acs.jpclett.7b03323
J. Phys. Chem. Lett. 2018, 9, 745−750

Notably, in many of our simulations (e.g., the $S_2C_6H_{12}$ case in Figure 4), the bimodal behavior of the conformations is reflected as a bimodal conductance for pulling distances close to the fully elongated molecule. This is due to the presence of two conformational groups: one in which one last gauche conformation is present, and a second one free of gauche defects.

The connection between molecular conformation and conductance, which makes molecular electronic experiments a useful witness of conformational dynamics, has also been recognized in different contexts. In ref 34 and ref 37, the authors studied the effects of molecular rotation and gauche conformations in the conductance of σ-bonded molecules, identifying gauche conformations as possibly responsible for the switching of the conductance during scanning tunneling microscopy (STM) experiments. Reference 26 suggests that different junction configurations can lead to multiple peaks in conductance histograms. In turn, ref 53 and ref 27 showed how the conductance changes with respect to the variation of the torsion angles in biphenyl systems. In particular, the decrease of the conductance of alkanes due to gauche defects has been attributed to interferences that arise due to the interaction between nonnearest neighbors in the molecular chain.[36] Our simulations in Figure S2 agree with this result. However, as shown in Figure S3a, the kinks observed in the transmission due to variation in the dihedral angles are not necessarily related to through space interactions that lead to quantum interference. In fact, the kinks survive even when the quantum interference effects are suppressed. This implies that, while interferences due to gauche conformers are clearly present, the kinks during pulling are best understood by examining changes in orbital level alignment as shown in Figure 3.

In conclusion, through simulations we have shown that the conductance profile during pulling of single-molecule junctions (before the conductance plateau where the molecule is fully elongated) contains valuable information about the conformational dynamics of the molecule and its interaction with the electrode. These insights enhance the information that can be extracted from molecular junction experiments and thus the utility of this class of measurements as a general route to develop multidimensional single-molecule spectroscopies.

Specifically, we performed pulling coupled to transport simulations of Au−S-$(CH_2)_n$-S-Au (n = 3−8) junctions, and considered different electrode shapes and pulling speeds. The simulations demonstrate that through-space coupling between the molecule and electrode is responsible for the overall decay of the conductance during pulling. This implies that the value of the conductance decay coefficient during pulling is sensitive to the precise shape of the electrodes and other factors that could affect the through-space interactions like the presence of solvent. In addition, the simulations show kinks in the transmission that are related to the variation of the backbone dihedral angles of the alkane chains. This structure-transport relation offers an efficient solution to experimentally monitor conformational dynamics at the single-molecule level. Further, the simulations clarify the physical origin of the dihedral-conductance connection. As shown, both quantum destructive interference and changes in molecular orbital's energies are present when changing these dihedrals. However, the latter one is dominant and responsible for the kinks in the conductance profile during pulling. Importantly, these results illustrate how molecular junction experiments can be used to probe nonequilibrium conformational ensembles that can be generated during pulling, with the favorable sensitivity offered by tunneling-based conductance measurements. Even when these results pertain to a particular class of molecular junctions, they illustrate the information content in this class of experiments and can be used as a starting point to interpret measurements in other molecules.

■ ASSOCIATED CONTENT

Supporting Information

The Supporting Information is available free of charge on the ACS Publications website at DOI: 10.1021/acs.jpclett.7b03323.

Analysis of the effect of through-space intramolecular and electrode−molecule interactions to the conductane profile during elongation (PDF)

■ AUTHOR INFORMATION

Corresponding Author

*E-mail: ignacio.franco@rochester.edu.

ORCID

Ignacio Franco: 0000-0002-0802-8185

Notes

The authors declare no competing financial interest.

■ ACKNOWLEDGMENTS

This material is supported by University of Rochester startup funds.

■ REFERENCES

(1) Datta, S. *Quantum Transport: Atom to Transistor*; Cambridge University Press: Cambridge, U.K., 2005.

(2) Cuevas, J. C.; Scheer, E. *Molecular Electronics: An Introduction to Theory and Experiment*; World Scientific: Singapore, 2017; *Vol. 15*.

(3) Aradhya, S. V.; Venkataraman, L. Single-Molecule Junctions Beyond Electronic Transport. *Nat. Nanotechnol.* **2013**, *8*, 399−410.

(4) Bruot, C.; Hihath, J.; Tao, N. Mechanically Controlled Molecular Orbital Alignment in Single Molecule Junctions. *Nat. Nanotechnol.* **2012**, *7*, 35−40.

(5) Xu, B. Q.; Li, X. L.; Xiao, X. Y.; Sakaguchi, H.; Tao, N. J. Electromechanical and Conductance Switching Properties of Single Oligothiophene Molecules. *Nano Lett.* **2005**, *5*, 1491−1495.

(6) Ismael, A. K.; Wang, K.; Vezzoli, A.; Al-Khaykanee, M. K.; Gallagher, H. E.; Grace, I. M.; Lambert, C. J.; Xu, B.; Nichols, R. J.; Higgins, S. J. Side-Group-Mediated Mechanical Conductance Switching in Molecular Junctions. *Angew. Chem.* **2017**, *129*, 15580−15584.

(7) Zhang, J.; Kuznetsov, A. M.; Medvedev, I. G.; Chi, Q.; Albrecht, T.; Jensen, P. S.; Ulstrup, J. Single-Molecule Electron Transfer in Electrochemical Environments. *Chem. Rev.* **2008**, *108*, 2737−2791.

(8) McCreery, R. L.; Bergren, A. J. Progress with Molecular Electronic Junctions: Meeting Experimental Challenges in Design and Fabrication. *Adv. Mater.* **2009**, *21*, 4303−4322.

(9) Díez-Pérez, I.; Hihath, J.; Lee, Y.; Yu, L.; Adamska, L.; Kozhushner, M. A.; Oleynik, I. I.; Tao, N. Rectification and Stability of a Single Molecular Diode with Controlled Orientation. *Nat. Chem.* **2009**, *1*, 635−641.

(10) Xiang, D.; Wang, X.; Jia, C.; Lee, T.; Guo, X. Molecular-Scale Electronics: From Concept to Function. *Chem. Rev.* **2016**, *116*, 4318−4440.

(11) Andergassen, S.; Meden, V.; Schoeller, H.; Splettstoesser, J.; Wegewijs, M. Charge Transport Through Single Molecules, Quantum Dots and Quantum Wires. *Nanotechnology* **2010**, *21*, 272001.

(12) Pistolesi, F.; Blanter, Y. M.; Martin, I. Self-Consistent Theory of Molecular Switching. *Phys. Rev. B* **2008**, *78*, 085127.

(13) Parker, S. M.; Smeu, M.; Franco, I.; Ratner, M. A.; Seideman, T. Molecular Junctions: Can Pulling Influence Optical Controllability? *Nano Lett.* **2014**, *14*, 4587−4591.

DOI: 10.1021/acs.jpclett.7b03323
J. Phys. Chem. Lett. 2018, 9, 745−750

(14) Rascón-Ramos, H.; Artés, J. M.; Li, Y.; Hihath, J. Binding Configurations and Intramolecular Strain in Single-Molecule Devices. *Nat. Mater.* **2015**, *14*, 517−522.
(15) Boese, D.; Schoeller, H. Influence of Nanomechanical Properties on Single-Electron Tunneling: A Vibrating Single-Electron Transistor. *EPL* **2001**, *54*, 668.
(16) Pobelov, I. V.; Mészáros, G.; Yoshida, K.; Mishchenko, A.; Gulcur, M.; Bryce, M. R.; Wandlowski, T. An Approach to Measure Electromechanical Properties of Atomic and Molecular Junctions. *J. Phys.: Condens. Matter* **2012**, *24*, 164210.
(17) Pirrotta, A.; De Vico, L.; Solomon, G. C.; Franco, I. Single-Molecule Force-Conductance Spectroscopy of Hydrogen-Bonded Complexes. *J. Chem. Phys.* **2017**, *146*, 092329.
(18) Joachim, G.; Gimzewski, J.; Aviram, A. Electronics Using Hybrid-Molecular and Mono-Molecular Devices. *Nature* **2000**, *408*, 541.
(19) Franco, I.; George, C. B.; Solomon, G. C.; Schatz, G. C.; Ratner, M. A. Mechanically Activated Molecular Switch Through Single-Molecule Pulling. *J. Am. Chem. Soc.* **2011**, *133*, 2242−2249.
(20) Alavi, S.; Larade, B.; Taylor, J.; Guo, H.; Seideman, T. Current-Triggered Vibrational Excitation in Single-Molecule Transistors. *Chem. Phys.* **2002**, *281*, 293−303.
(21) Koch, J.; Semmelhack, M.; von Oppen, F.; Nitzan, A. Current-Induced Nonequilibrium Vibrations in Single-Molecule Devices. *Phys. Rev. B* **2006**, *73*, 155306.
(22) Chen, F.; Li, X.; Hihath, J.; Huang, Z.; Tao, N. Effect of Anchoring Groups on Single-Molecule Conductance: Comparative Study of Thiol-, Amine-, and Carboxylic-Acid-Terminated Molecules. *J. Am. Chem. Soc.* **2006**, *128*, 15874−15881.
(23) Engelkes, V. B.; Beebe, J. M.; Frisbie, C. D. Length-Dependent Transport in Molecular Junctions Based on SAMs of Alkanethiols and Alkanedithiols: Effect of Metal Work Function and Applied Bias on Tunneling Efficiency and Contact Resistance. *J. Am. Chem. Soc.* **2004**, *126*, 14287−14296.
(24) Xu, B.; Tao, N. J. Measurement of Single-Molecule Resistance by Repeated Formation of Molecular Junctions. *Science* **2003**, *301*, 1221−1223.
(25) Lindsay, S. M.; Ratner, M. A. Molecular Transport Junctions: Clearing Mists. *Adv. Mater.* **2007**, *19*, 23−31.
(26) Li, C.; Pobelov, I.; Wandlowski, T.; Bagrets, A.; Arnold, A.; Evers, F. Charge Transport in Single Au|Alkanedithiol|Au Junctions: Coordination Geometries and Conformational Degrees of Freedom. *J. Am. Chem. Soc.* **2008**, *130*, 318−326.
(27) Mishchenko, A.; Vonlanthen, D.; Meded, V.; Burkle, M.; Li, C.; Pobelov, I. V.; Bagrets, A.; Viljas, J. K.; Pauly, F.; Evers, F.; Mayor, M.; Wandlowski, T. Influence of Conformation on Conductance of Biphenyl-Dithiol Single-Molecule Contacts. *Nano Lett.* **2010**, *10*, 156−163.
(28) Wold, D. J.; Frisbie, C. D. Fabrication and Characterization of Metal-Molecule-Metal Junctions by Conducting Probe Atomic Force Microscopy. *J. Am. Chem. Soc.* **2001**, *123*, 5549−5556.
(29) Cui, X.; Primak, A.; Zarate, X.; Tomfohr, J.; Sankey, O.; Moore, A. L.; Moore, T. A.; Gust, D.; Nagahara, L.; Lindsay, S. Changes in The Electronic Properties of a Molecule When it is Wired Into a Circuit. *J. Phys. Chem. B* **2002**, *106*, 8609−8614.
(30) Lee, T.; Wang, W.; Klemic, J. F.; Zhang, J. J.; Su, J.; Reed, M. A. Comparison of Electronic Transport Characterization Methods for Alkanethiol Self-Assembled Monolayers. *J. Phys. Chem. B* **2004**, *108*, 8742−8750.
(31) Wang, W.; Lee, T.; Reed, M. A. Elastic and Inelastic Electron Tunneling in Alkane Self-Assembled Monolayers. *J. Phys. Chem. B* **2004**, *108*, 18398−18407.
(32) Akkerman, H. B.; de Boer, B. Electrical Conduction Through Single Molecules and Self-Assembled Monolayers. *J. Phys. Condens. Matter* **2008**, *20*, 013001.
(33) Cui, X.; Zarate, X.; Tomfohr, J.; Sankey, O.; Primak, A.; Moore, A. L.; Moore, T. A.; Gust, D.; Harris, G.; Lindsay, S. Making Electrical Contacts to Molecular Monolayers. *Nanotechnology* **2002**, *13*, 5.
(34) Paulsson, M.; Krag, C.; Frederiksen, T.; Brandbyge, M. Conductance of Alkanedithiol Single-Molecule Junctions: A Molecular Dynamics Study. *Nano Lett.* **2009**, *9*, 117−121.
(35) Lin, J.; Beratan, D. N. Tunneling While Pulling: the Dependence of Tunneling Current on End-to-End Distance in a Flexible Molecule. *J. Phys. Chem. A* **2004**, *108*, 5655−5661.
(36) Solomon, G. C.; Herrmann, C.; Hansen, T.; Mujica, V.; Ratner, M. A. Exploring Local Currents in Molecular Junctions. *Nat. Chem.* **2010**, *2*, 223−228.
(37) Tagami, K.; Tsukada, M. Conductance Switching of Alkane Molecules by Gauche Conformation on Au(111). *e-J. Surf. Sci. Nanotechnol.* **2004**, *2*, 186−190.
(38) Hutcheson, J.; Franco, I.; Nicolas, R.; Carignano, M.; Ratner, M. A.; Schatz, G. C. TRANSpull: computes pulling coupled to transport properties of single molecules. 2011; https://nanohub.org/resources/11739.
(39) Ponder, J. W. *TINKER: Software Tools for Molecular Design*; Washington University School of Medicine: Saint Louis, MO, 2004, 3.
(40) Beeman, D. Some Multistep Methods for Use in Molecular Dynamics Calculations. *J. Comput. Phys.* **1976**, *20*, 130−139.
(41) Levitt, M. Molecular Dynamics of Native Protein: I. Computer Simulation of Trajectories. *J. Mol. Biol.* **1983**, *168*, 595−617.
(42) Nosé, S. A Unified Formulation of the Constant Temperature Molecular Dynamics Methods. *J. Chem. Phys.* **1984**, *81*, 511−519.
(43) Nosé, S. A Molecular Dynamics Method for Simulations in the Canonical Ensemble. *Mol. Phys.* **1984**, *52*, 255−268.
(44) Hoover, W. G. Canonical Dynamics: Equilibrium Phase-Space Distributions. *Phys. Rev. A* **1985**, *31*, 1695.
(45) Allinger, N. L.; Yuh, Y. H.; Lii, J. H. Molecular Mechanics. The MM3 Force Field for Hydrocarbons. 1. *J. Am. Chem. Soc.* **1989**, *111*, 8551−8566.
(46) Lii, J. H.; Allinger, N. L. Molecular Mechanics. The MM3 Force Field for Hydrocarbons. 2. Vibrational Frequencies and Thermodynamics. *J. Am. Chem. Soc.* **1989**, *111*, 8566−8575.
(47) Lii, J. H.; Allinger, N. L. Molecular Mechanics. The MM3 Force Field for Hydrocarbons. 3. The Van der Waals' Potentials and Crystal Data for Aliphatic and Aromatic Hydrocarbons. *J. Am. Chem. Soc.* **1989**, *111*, 8576−8582.
(48) Gottschalck, J.; Hammer, B. A Density Functional Theory Study of the Adsorption of Sulfur, Mercapto, and Methylthiolate on Au(111). *J. Chem. Phys.* **2002**, *116*, 784−790.
(49) Carey, R.; Chen, L.; Gu, B.; Franco, I. When Can Time-Dependent Currents Be Reproduced by the Landauer Steady-State Approximation? *J. Chem. Phys.* **2017**, *146*, 174101.
(50) Scheer, E. *Molecular Electronics: An Introduction to Theory and Experiment*; World Scientific: Singapore, 2010; *Vol. 1*.
(51) Hoffmann, R. An Extended Hückel Theory. I. Hydrocarbons. *J. Chem. Phys.* **1963**, *39*, 1397−1412.
(52) Verzijl, C.; Seldenthuis, J.; Thijssen, J. Applicability of the wide-Band Limit in DFT-Based Molecular Transport Calculations. *J. Chem. Phys.* **2013**, *138*, 094102.
(53) Venkataraman, L.; Klare, J. E.; Nuckolls, C.; Hybertsen, M. S.; Steigerwald, M. L. Dependence of Single-Molecule Junction Conductance on Molecular Conformation. *Nature* **2006**, *442*, 904−907.

■ NOTE ADDED AFTER ASAP PUBLICATION

This paper was published ASAP on February 1, 2018. Figures 2 and 3 were updated. The revised paper was reposted on February 7, 2018.

DOI: 10.1021/acs.jpclett.7b03323
J. Phys. Chem. Lett. 2018, 9, 745−750